Biophysical Chemistry 195 (2014) 22–31

Contents lists available at ScienceDirect

Biophysical Chemistry

journal homepage: http://www.elsevier.com/locate/biophyschem

A thermodynamic investigation of the glucose-6-phosphate isomerization

Philip Hoffmann [a], Christoph Held [a,*], Thomas Maskow [b], Gabriele Sadowski [a]

[a] Laboratory of Thermodynamics, Department of Biochemical and Chemical Engineering, TU Dortmund, Emil-Figge-Str. 70, 44227 Dortmund, Germany
[b] Department of Environmental Microbiology, UFZ Centre for Environmental Research Leipzig-Halle GmbH, Permoserstr. 15, 04318 Leipzig, Germany

HIGHLIGHTS

- Equilibrium constant K strongly depends on G6P concentration for G6P ↔ F6P reaction.
- $\Delta^R g^+$ upon using either K_a or K_m differs by up to 30%.
- Activity-coefficient ratio of G6P and F6P strongly deviates from unity.
- Activity-coefficient ratio K_γ could be predicted with ePC-SAFT accurately.
- Influence of buffer and glutamate on K_γ could be predicted with ePC-SAFT accurately.

GRAPHICAL ABSTRACT

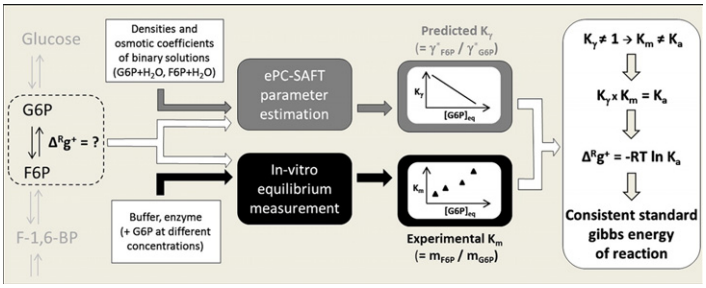

ARTICLE INFO

Article history:
Received 24 June 2014
Received in revised form 7 August 2014
Accepted 9 August 2014
Available online 21 August 2014

Keywords:
Thermodynamic equilibrium constant
Activity coefficient
Gibbs energy of reaction
Enthalpy of reaction
ePC-SAFT
Glycolysis

ABSTRACT

In this work, $\Delta^R g^+$ values for the enzymatic G6P isomerization were determined as a function of the G6P equilibrium molality between 25 °C and 37 °C. The reaction mixtures were buffered at pH = 8.5. In contrast to standard literature work, $\Delta^R g^+$ values were determined from activity-based equilibrium constants instead of molality-based apparent values. This yielded a $\Delta^R g^+$ value of 2.55 ± 0.05 kJ mol^{-1} at 37 °C, independent of the solution pH between 7.5 and 8.5. Furthermore, $\Delta^R h^+$ was measured at pH = 8.5 and 25 °C yielding 12.05 ± 0.2 kJ mol^{-1}.
Accounting for activity coefficients turned out to influence $\Delta^R g^+$ up to 30% upon increasing the G6P molality. This result was confirmed by predictions using the thermodynamic model ePC-SAFT.
Finally, the influence of the buffer and of potassium glutamate as an additive on the reaction equilibrium was measured and predicted with ePC-SAFT in good agreement.

1. Introduction

One of the most obvious characteristics that distinguishes chemical from biological systems is the diversity of the species involved. A biological process often involves parts of a metabolic network inside a complex organism with numerous reactants, products, enzymes, and other biological compounds that are often largely undefined with respect to concentration and their physical properties. Even more complex, some of these compounds are present as different species, depending on solution conditions such as pH (degree of protonation) and Mg concentrations (degree of complex formation) [1]. While sequences of chemical reactions are already predictable, the thermodynamics of biological-reaction sequences is still in its infancy [1]. The species diversity and, even more important, the lack of knowledge of the physical properties of biological compounds and mixtures have

* Corresponding author at: Emil-Figge-Str. 70, 44227 Dortmund, Germany. Tel.: +49 2317552086; fax: +49 2317552572.
E-mail address: christoph.held@bci.tu-dortmund.de (C. Held).

http://dx.doi.org/10.1016/j.bpc.2014.08.002
0301-4622/

long been a drawback in the rational and efficient design of biological processes.

Several methods have recently been developed for the thermodynamic characterization of biological processes [2–9]. A thermodynamic key quantity applied in these methods, some of which are referred to as feasibility studies [10–13], is the standard Gibbs energy of reaction $\Delta^R g^+$. Thermodynamically correct, this $\Delta^R g^+$ has to be calculated from the activity-based (thermodynamic) equilibrium constant of a reaction, K_a. In the standard literature however, $\Delta^R g^+$ is usually calculated from the molality-based (apparent) equilibrium constant K_m (also referred to as K′), which is thermodynamically incorrect.

K_m can be converted into K_a as long as the activity coefficients of the reactants and products are known at reaction conditions. The activity coefficient describes the deviations of the reactants and products from their standard state (e.g., infinite dilution), caused by interactions between all present compounds in the reaction mixture at finite concentrations. These interactions include molecular interactions of the reactants and products with system compounds that do not directly take part in the reaction and interactions among the reacting compounds themselves. Therefore, the activity coefficients do not only depend on the presence and the nature of the system compounds but also directly on the reactant and product concentration. Furthermore, the system compounds may build complexes or may protonate/deprotonate depending on solution conditions such as pH, which additionally influences activity coefficients.

Unfortunately, data on species activity coefficients in biological systems is scarce and their influence on thermodynamic properties such as $\Delta^R g^+$ is largely unknown. Accordingly, the influence of activity coefficients is usually neglected for the characterization of biological reactions [14]. In our previous work, the importance to account for activity coefficients in order to characterize biological reactions was soundly demonstrated [15]. For the considered reaction in that work (hydrolysis of methyl ferulate), it was shown that the activity coefficients of the reacting agents strongly deviate from unity and thus have a large impact on $\Delta^R g^+$ values.

In this work, the reaction equilibrium of the enzymatic isomerization of glucose-6-phosphate (G6P) to fructose-6-phosphate (F6P) (Eq. (1)) was investigated.

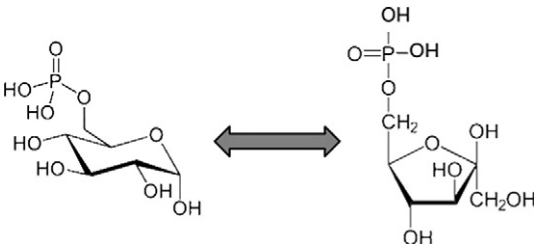

(1)

The isomerization is catalyzed by the enzyme phosphoglucose isomerase (PGI). The G6P isomerization is the second step of glycolysis, the central carbon degradation pathway in any organism. A thorough understanding of this reaction is thus required for many biotechnological processes. Following the procedure in our previous study [15], the (thermodynamic) activity-based equilibrium constant K_a was determined by measuring the molality-based (apparent) equilibrium constant K_m at different G6P molalities and extrapolating K_m to zero G6P molality. In addition, the influence of reaction additives on the G6P isomerization equilibrium was investigated.

Next to K_a (and $\Delta^R g^+$ values calculated thereof), also the standard enthalpy of reaction ($\Delta^R h^+$) is a fundamental thermodynamic quantity required for the characterization of reactions and for the operation, design, and optimization of biochemical processes. ITC (isothermal titration calorimetry) has already proven its capability to determine physicochemical properties (molecular interactions) and reaction enthalpies for the characterization of biochemical processes [16–18]. In this work, $\Delta^R h^+$ was measured using ITC. In addition, these $\Delta^R h^+_{ITC}$ values were compared to $\Delta^R h^+$ values obtained by applying the van't Hoff equation to the temperature-dependent K_a values determined from equilibrium measurements in this work. This way, $\Delta^R h^+_{ITC}$ can be used to verify the accuracy of the K_a values (and thus of $\Delta^R g^+$) obtained from K_m measurements.

Another evidence for the quality of the experimentally-determined K_a values can be obtained by comparing with those predicted via K_m and activity coefficients obtained from thermodynamic models. In the past decades, researchers started to develop thermodynamic models in order to describe activity coefficients in biological solutions. The Pitzer equation is one of the most famous correlative models [19]. The availability of those models allows calculating activity coefficients depending on temperature, solutes, and solute molalities. One disadvantage of models like the Pitzer equation is the need for solute–solute parameters. Setting them to zero (as for predictions) means that solute–solute interactions are completely neglected, which leads to inaccurate modeling results [20]. Thus, such models are usually not able to quantitatively predict activity coefficients in multi-solute solutions.

However, there are advanced thermodynamic models that allow for quantitative predictions of activity coefficients in biological systems. One example is the Statistical Associating Fluid Theory (SAFT) and models based on SAFT. They are able to account for specific interactions between biological compounds caused by hydrogen bonding or charges. In this work, the activity coefficients were estimated by the electrolyte Perturbed-Chain SAFT (ePC-SAFT) [21]. This model is especially suitable for aqueous solutions containing biomolecules and electrolytes [21–29]. It has already successfully been used for predictions of activity coefficients in multi-solute solutions based only on model parameters fitted to properties of pure compounds and binary solute + solvent solutions.

2. Thermodynamic formalism for the G6P isomerization

This section describes the formalism for a thermodynamically consistent description of the isomerization of G6P to F6P (Eq (1)). Both compounds were used as dipotassium salts $G6PK_2$ and $F6PK_2$ in this study. The reacting agents of Eq. (1) are thus not G6P and F6P, but rather the twofold deprotonated species, denoted with $G6P^{2-}$ and $F6P^{2-}$ in the following. These species were exclusively present at reaction conditions as the chosen pH of 8.5 is significantly above the highest pK_a of G6P and F6P [30], i.e. the compounds were completely dissociated. Moreover, ion pairing between $G6P^{2-}$ and K^+ as well as between $F6P^{2-}$ and K^+ was not assumed to occur as the considered concentrations of $G6PK_2$ and $F6PK_2$ were very small (in the mmolal range). The thermodynamic equilibrium constant K_a of the G6P isomerization at these conditions is defined as

$$K_a = \frac{a^{eq}_{F6P^{2-}}}{a^{eq}_{G6P^{2-}}} \tag{2}$$

where a^{eq} are the equilibrium activities of the reacting species. The thermodynamic activity is defined as the product of concentration and respective activity coefficient, which itself depends on the standard state and on the concentration unit used:

$$a_i = m_i \cdot \gamma_i^{*,m}. \tag{3}$$

In this work, the concentration is reported as molality m_i (moles of compound i per kg water). The use of molality is recommended for thermodynamic considerations, as the reference (kg of pure water) is a temperature-independent property, which is not true for molarity (mol L^{-1}) or concentration (g L^{-1}). The standard state for the molality-based activity coefficient $\gamma_i^{*,m}$ is a hypothetical solution of compound i in water, which is defined as a one molal solution that exhibits the same interactions as at infinite dilution. The activity coefficient $\gamma_i^{*,m}$ is preferably used for solutes that are present at very low molalities in the reaction mixture (dilute solution). As $G6PK_2$ and

$F6PK_2$ were used at low molalities in the experiments, $\gamma_i^{*,m}$ was used in this work.

In an analogous manner, the thermodynamic equilibrium constant K_a can be written as

$$K_a = K_m \cdot K_\gamma \tag{4}$$

where K_m is usually calculated from experimental equilibrium molalities the reacting species. The ratio of product and reactant activity coefficient (K_γ) is calculated from the respective molality-based activity coefficients. For the G6P isomerization, K_m and K_γ become

$$K_m = \frac{m^{eq}_{F6P^{2-}}}{m^{eq}_{G6P^{2-}}} \tag{5}$$

and

$$K_\gamma = \frac{\gamma^{*,m}_{F6P^{2-}}}{\gamma^{*,m}_{G6P^{2-}}}. \tag{6}$$

At infinite dilution of $G6P^{2-}$ and $F6P^{2-}$, the activity coefficients $\gamma^{*,m}_{G6P^{2-}}$ and $\gamma^{*,m}_{F6P^{2-}}$ become unity. According to Eq. (6), also K_γ becomes unity at these conditions. For this reason, the thermodynamic equilibrium constant K_a can be determined from experimental K_m values, extrapolated to infinitely low $G6P^{2-}$ and $F6P^{2-}$ equilibrium molalities. The extrapolation will be shown in Fig. 1.

The availability of K_a values calculated from Eq. (4) allows determining the standard Gibbs energy of reaction $\Delta^R g^+$ (Eq. (7)).

$$\Delta^R g^+ = -RT \ln K_a \tag{7}$$

Unlike K_a, the quantities K_m and K_γ may depend on the reactant and product molalities and on the presence of additives (e.g., buffer or salts) in the reaction mixture. Consequently, the reactant and product activity coefficients may depend on additives and must be considered in the analysis of additive-containing reaction mixtures. In this work, an analysis was performed to investigate the influence of the buffer Tris–HCl and of potassium glutamate (KGlu) on the G6P isomerization equilibrium.

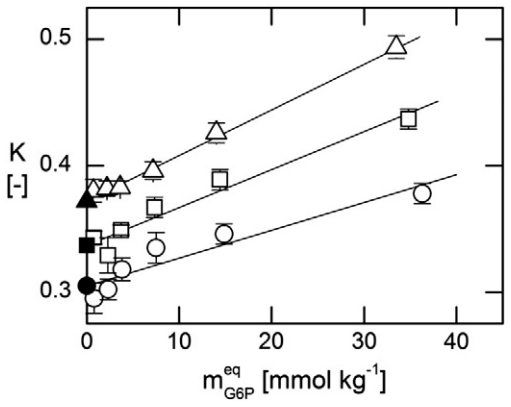

Fig. 1. Experimental K_m values (pH 8.5) for the isomerization of glucose-6-phosphate at 25 °C (open circles), 30 °C (open squares), and 37 °C (open triangles) as function of the $G6P^{2-}$ equilibrium molality, calculated according to Table 2 and Eq. (5). The full symbols represent K_a values, which were obtained by extrapolating the K_m values to $m^{eq}_{G6P} = 0$ mmol kg^{-1} (the lines are shown to guide the eye).

3. Experimental work

3.1. Materials

All of the relevant information on the substances used in this study is given in Table 1. The substances were used as obtained without further purification. The reaction was catalyzed enzymatically by a G6P isomerase (GPI, EC 5.3.1.9) from *Saccharomyces cerevisiae* (Megazyme International, Bray, Ireland). According to the supplier, the enzyme activity for G6P was 350 Units mg^{-1}.

3.2. Measurement of K_m values

The equilibrium molalities of the reacting agents (required to determine K_m) were measured in double-walled 5-ml glass reactors. These measurements were all carried out at 25 °C, 30 °C, and 37 °C at initial $G6PK_2$ molalities of 1 mmol kg^{-1} < $m^{init}_{G6PK_2}$ < 50 mmol kg^{-1}. Each regular reaction mixture was prepared using a Tris–HCl buffer (0.05 mol kg^{-1}), adjusted to pH 8.5 (due to the high biological enzyme activity at this pH according to the supplier) with hydrochloric acid (HCl). To investigate the influence of the buffer molality at constant pH, the Tris molality was varied between 0.01 and 0.5 mol kg^{-1}. To investigate the influence of the solution pH at a constant Tris molality, the pH was adjusted to pH 7.5 (by increasing the amount of HCl added).

It has to be mentioned that the enzyme activity was not determined in this work. Rather, the recommended conditions for the PGI enzyme (pH optimum: 8.5, temperature optimum: 30 °C) were applied in this work. In preliminary tests to this work it was ensured (1) that enough enzyme was available for catalyzing the reaction and (2) that enough time was allowed to obtain equilibrium conditions.

The temperature of the reaction mixtures was adjusted using a C12 CP Lauda thermostat (Lauda, Lauda-Königshofen, Germany) with an accuracy of ±0.1 K. This was controlled with temperature sensors (Pt 100) that were placed directly in the reaction solution. Each reactor was equipped with septum-containing caps in order to add the enzyme solution with a 0.1 ml syringe. The enzyme solution was prepared by dissolving the lyophilized enzyme PGI in a Tris solution with the same Tris molality as for the respective $G6PK_2$/Tris solution and equilibrated at reaction temperature (25 °C, 30 °C, 37 °C) prior to addition. Preliminary tests (data not provided here) have shown that an enzyme concentration of 0.255 Units ml^{-1} was suitable to reach thermodynamic equilibrium within a reasonable time frame (one to 5 h depending on the initial $G6PK_2$ molality, also for measurements at pH 7.5). To ensure homogeneity, the reaction mixture was continuously stirred at moderate speed (300 rpm) using a magnetic stirrer. An investigation on the stirring procedure revealed that the K_m values were independent of the stirring speed (data not shown).

Table 1
Substances used in this work, including the respective Chemical Abstracts Service (CAS) registry number, empirical formula, supplier (M = Merck KGaA, S = Sigma Aldrich Chemie GmbH), and the approximate anhydrous mass-fraction purity as provided by the supplier.

Substance	CAS-no.	Formula	Supplier	Purity
Fructose-6-phosphate dipotassium salt	103213-47-4	$C_6H_{11}O_9PK_2$	S	≥0.97
Glucose-6-phosphate dipotassium salt hydrate	5996-17-8	$C_6H_{11}O_9PK_2 \cdot xH_2O$	S	≥0.98
Glutamate (monopotassium salt)	6382-01-0	$C_5H_8KNO_4$	S	>0.99
Hydrochloric acid	7647-01-0	HCl	M	–
Sodium acetate	127-09-3	$C_2H_3NaO_2$	S	>0.99
Sodium hydroxide	1310-73-2	NaOH	M	–
Trizma® base	77-86-1	$C_4H_{11}NO_3$	S	>0.998

$2 < x < 4$.

Prior to chromatographic analysis, the samples were centrifuged in ultrafiltration units (10 kDa) with a 'Universal 32R' centrifuge (Hettich, Tuttlingen, Germany) at 14,000 *g*. By this, the enzyme was separated from $G6P^{2-}$ and $F6P^{2-}$ in order to prevent an equilibrium shift. The centrifugation process took max. 10 min; as the centrifugation temperature was set to the respective reaction temperature (25 °C, 30 °C, 37 °C) equilibrium shifts could be avoided.

In this work also the influence of potassium glutamate (KGlu) as an additive on the reaction equilibrium was investigated. The measurements with additional KGlu were performed as described above except that KGlu was dissolved in the $G6PK_2$/Tris solution prior to enzyme addition. KGlu was added in the range $0.05 < \text{mol kg}^{-1}\ \text{KGlu} < 1$. These measurements were all carried out at 37 °C and $m^{init}_{G6PK_2} = 0.05\ \text{mol kg}^{-1}$.

All solutions were gravimetrically prepared using a Sartorius CPA324S balance (Sartorius, Göttingen, Germany) with an accuracy of $\pm 10^{-4}$ g. The resulting K_m values reported in Sections 1 and 5.3 are averages of at least three independent repetitions (i.e. three independently prepared reaction mixtures).

3.3. HPLC analysis

An Agilent series 1200 HPLC (Agilent, Böblingen, Germany) equipped with an electrochemical detector Decade II (ERC GmbH, Riemerling, Germany) was used to quantify the molalities of $G6P^{2-}$ and $F6P^{2-}$ after equilibrium was reached. $G6P^{2-}$ and $F6P^{2-}$ were separated with a CarboPac PA1 carbohydrate column, 4 × 250 mm (Fisher Scientific GmbH, Schwerte, Germany), at a flow rate of 1 ml min^{-1}. Aqueous solutions of sodium hydroxide and sodium acetate were used as mobile phases in a gradient mode according to [31]. The detection was carried out by pulsed amperometry with the following potential (E_i)–time (t_i) sequence: $E_1 = 150$ mV, $t_1 = 200$ ms; $E_2 = 650$ mV, $t_2 = 400$ ms; and $E_3 = -750$ mV, $t_3 = 200$ ms. Each mixture was analyzed by drawing at least two samples out of the reaction mixture.

3.4. Measurement of $\Delta^R h^+$ values

This section gives a brief description of the calorimetric experiments carried out in this study. Detailed information on isothermal titration experiments can be found in the literature (e.g. [16]).

The standard enthalpy of reaction $\Delta^R h^+$ of the G6P isomerization was measured calorimetrically using a TAM III nanocalorimeter (TA Instruments, New Castle, USA) with a precision of ±200 nW. The experimental setup consisted of a reaction ampule and a reference ampule to balance the heat capacity of the ampules. Both ampules were filled with $G6PK_2$/Tris solutions and placed in the calorimeter to equilibrate the solutions at reaction temperature (25 °C). A 250 μl syringe was filled with the enzyme solution and placed nearby the calorimeter so that the cannula extended into the reaction ampule inside the calorimeter. The substrate and the enzyme solution were prepared in the same way (under the same conditions) as for the equilibrium measurements in the glass reactors (Section 3.2).

The reaction was started upon titration of the buffered enzyme solution in the reaction ampule containing the $G6PK_2$/Tris solution. During the reaction, the solutions in both, reaction and reference ampule, were continuously stirred. Prior to chromatographic analysis, the samples were centrifuged in ultrafiltration units (10 kDa) with a 'Universal 32R' centrifuge (Hettich, Tuttlingen, Germany) at 14,000 *g* to separate the enzyme from $G6P^{2-}$ and $F6P^{2-}$ and to prevent an equilibrium shift. The actual quantity recorded by the calorimeter is the heat absorbed during the reaction (given in Joule per second). The final result, $\Delta^R h^+_{ITC}$, was obtained by integrating the heat curve over the reaction time and dividing this value by the number of moles $G6P^{2-}$ converted. The resulting value for $\Delta^R h^+_{ITC}$ reported in Section 1 is the average of three independent repetitions.

4. Modeling with ePC-SAFT

In this work the $G6P^{2-}$ and $F6P^{2-}$ activity coefficients were predicted with ePC-SAFT. The model calculates the residual Helmholtz energy of a system as the sum of different independent contributions (Eq. (8)):

$$a^{res} = a^{hc} + a^{disp} + a^{assoc} + a^{ion}. \tag{8}$$

The hard chain contribution (a^{hc}) represents the repulsion of molecules. The dispersion term (a^{disp}) accounts for the attractive dispersion forces (e.g. van der Waals) among molecules and the association term (a^{assoc}) accounts for the formation of hydrogen bonds between associating molecules which are considered to have a certain number of association sites N_i^{assoc}. A molecule is assumed to consist of m_i^{seg} spherical segments of diameter σ_i. The dispersion forces among the molecules are characterized by the dispersion-energy parameter u_i/k_B. The interaction between two associating molecules is represented by the association-energy parameter ε^{AiBi}/k_B. The interaction volume for association is accounted for by the association-volume parameter κ^{AiBi}.

In this work, expressions for the contributions a^{hc}, a^{disp}, and a^{assoc} were used as in the original PC-SAFT model [24]. The energy contribution for charged species (a^{ion}) was accounted for by a Debye–Hückel term (ePC-SAFT) according to [21]. By applying textbook thermodynamic relationships (see, e.g., [25]), any thermodynamic property of interest, e.g. density, osmotic coefficient, and activity coefficient, can be derived once the expression for a^{res} is known.

To predict activity coefficients in multi-component solutions, ePC-SAFT requires five pure-component parameters for each compound involved in the reaction mixtures as well as binary interaction parameters. All these parameters are already available for many compounds and mixtures; however, they were not yet available for some of the biological compounds/species considered in this work ($G6P^{2-}$, $F6P^{2-}$, Tris, Tris–H^+, and KGlu). For the parameter estimation of such biological compounds, experimental densities and osmotic coefficients of aqueous solutions have shown to be a suitable data basis (e.g. [26]). Thus, these data was measured in this work and used for the parameter estimation (see Appendix A for details). The resulting parameters are listed in Table 4 in Appendix A.

5. Results & discussion

5.1. Experimental determination of K_a, $\Delta^R g^+$, and $\Delta^R h^+$

5.1.1. Determination of K_m and K_a

The thermodynamic equilibrium constant K_a cannot be measured directly. However, according to Eq. (4), it is related to the experimentally accessible K_m values. In fact, K_a equals K_m in case that K_γ becomes unity. According to the definition of the $G6P^{2-}$ and $F6P^{2-}$ activity coefficients (see Section 2), K_γ becomes unity for an infinite dilution of $G6P^{2-}$ and $F6P^{2-}$ in water. Thus, K_a was obtained by measuring K_m at different $G6P^{2-}$ equilibrium molalities ($0.7 < \text{mmol } G6P^{2-}\ \text{kg}^{-1} < 36$) and extrapolating these K_m values to zero $G6P^{2-}$ molality. The corresponding equilibrium molalities at 25 °C, 30 °C, and 37 °C are reported in Table 2.

Fig. 1 shows the experimental K_m values from Table 2 as function of the $G6P^{2-}$ equilibrium molality. It can be observed that the K_m values significantly depend on the $G6P^{2-}$ molality m^{eq}_{G6P}. Irrespective of the temperature, K_m increases up to 30% when m^{eq}_{G6P} is increased from 0.7 to 33 mmol kg^{-1} and is highest ($K_m = 0.494$) at $m^{eq}_{G6P} = 33\ \text{mmol kg}^{-1}$ (at 37 °C). This clearly indicates that K_m of G6P isomerization cannot be treated as a constant universally-valid value. Thus, the corresponding molalities need to be reported when reporting K_m values of such biological reactions.

The extrapolation of K_m to $m^{eq}_{G6P} = 0\ \text{mmol kg}^{-1}$ yielded K_a values of 0.305 (25 °C), 0.337 (30 °C), and 0.372 (37 °C), respectively.

Table 2
Equilibrium molalities (in mmol kg^{-1}) of $F6P^{2-}$ at different $G6P^{2-}$ equilibrium molalities and temperatures, together with the molalities of the additional compounds of each reaction batch (buffer species Tris, Tris–H^+, and Cl^- as well as K^+ ions). The experimental K_m value is also shown.

batch	T °C	$G6P^{2-}$ mmol kg^{-1}	$F6P^{2-}$ mmol kg^{-1}	K^{+} [a] mmol kg^{-1}	Tris [b] mmol kg^{-1}	Tris–H^{+} [b] mmol kg^{-1}	Cl^{-} [b] mmol kg^{-1}	K_m [c] –
1	25	0.77	0.23	2.01	33.44	16.77	16.23	0.295
	30	0.75	0.26	2.01	33.42	16.76	16.12	0.343
	37	0.73	0.27	1.99	33.22	16.66	16.04	0.380
2	25	2.31	0.70	6.01	33.44	16.77	16.23	0.302
	30	2.26	0.74	6.01	33.42	16.76	16.12	0.329
	37	2.17	0.83	6.00	33.22	16.66	16.04	0.382
3	25	3.80	1.21	10.01	33.44	16.77	16.23	0.318
	30	3.71	1.30	10.01	33.42	16.76	16.12	0.349
	37	3.61	1.38	9.99	33.27	16.68	16.09	0.383
4	25	7.50	2.51	20.02	33.44	16.77	16.23	0.335
	30	7.32	2.69	20.01	33.42	16.76	16.12	0.367
	37	7.16	2.83	19.99	33.27	16.68	16.09	0.396
5	25	14.85	5.14	39.97	33.32	16.71	16.10	0.346
	30	14.40	5.61	40.02	33.56	16.83	16.33	0.389
	37	14.03	5.98	40.02	33.27	16.68	16.09	0.426
6	25	36.29	13.72	100.02	33.32	16.71	16.10	0.378
	30	34.80	15.21	100.02	33.56	16.83	16.33	0.437
	37	33.47	16.54	100.02	33.27	16.68	16.09	0.494

[a] Obtained from mass balance calculations.
[b] Species constituting the buffer in this work. The initial Tris and HCl molalities were adjusted gravimetrically. At pH = 8.5 the buffer Tris–HCl (pK_a = 8.3 according to [30]) appeared in the deprotonated species (Tris) and in the protonated species (Tris–H^+) in the reaction mixture according to the Tris buffer equilibrium. The species molalities are required for the application of ePC-SAFT as reported in Section 5.2.
[c] Calculated according to Eq. (5).

5.1.2. Determination of $\Delta^R g^+$

In the literature, $\Delta^R g^+$ is usually determined from apparent K_m values (as determined in this work or as published in, e.g., the NIST database for enzyme-catalyzed reaction [32]). Following this and using K_m, e.g. of reaction batch No. 6 in Table 2 (K_m = 0.494) yields $\Delta^R g^+$ (37 °C) = 1.82 kJ mol^{-1}.

In contrast, $\Delta^R g^+$ calculated from Eq. (7) using K_a as obtained from Fig. 1 yields $\Delta^R g^+$ (37 °C) = 2.55 ± 0.05 kJ mol^{-1}. It is obvious, that K_m-based and K_a-based $\Delta^R g^+$ values deviate up to 30% at these conditions. Considering the results shown in Fig. 1, the difference in K_m-based and K_a-based $\Delta^R g^+$ values becomes the more pronounced the higher the $G6P^{2-}$ molality is. Accordingly, the potential error in the determination of $\Delta^R g^+$ caused by using K_m instead of K_a is certainly not negligible.

5.1.3. Determination of $\Delta^R h^+$

$\Delta^R h^+$ of the G6P isomerization was measured directly using ITC at 25 °C, pH 8.5, and $m^{init}_{G6PK_2}$ = 10 mmol kg^{-1}. The value obtained by ITC is $\Delta^R h^+_{ITC}$ = 12.05 ± 0.2 kJ mol^{-1}. This value can be compared to the one obtained from temperature-dependent K_a values (obtained from Fig. 1) according to the van't Hoff equation (Eq. (9)):

$$\frac{d \ln K_a}{d (1/T)} = \frac{\Delta^R h^+_{vH}}{R} \tag{9}$$

where T is the absolute temperature [in K], and R is the ideal-gas constant.

Using the temperature-dependent K_a values from Fig. 1 (0.305 at 25 °C, 0.337 at 30 °C, and 0.372 at 37 °C) in Eq. (9) yields $\Delta^R h^+_{vH}$ = 12.25 ± 0.3 kJ mol^{-1}. Both values, $\Delta^R h^+_{vH}$ and $\Delta^R h^+_{ITC}$ are in excellent agreement with a relative deviation of less than 2%. This demonstrates the reliability and the reasonability of the K_a values obtained by the procedure shown in Fig. 1.

5.1.4. Comparison of $\Delta^R h^+$ and $\Delta^R g^+$ measured in this work with literature values

The comparison of our own reaction equilibria data ($\Delta^R g^+$ and $\Delta^R h^+$) with literature data shows a diverse picture. Whereas standard literature (e.g. [40]) reports $\Delta^R g^+$ values between 1.6 kJ mol^{-1} and 1.8 kJ mol^{-1}, Dyson et al. [41] found a $\Delta^R g^+$ of 2.67 kJ mol^{-1}, which is very similar compared to our work (2.55 kJ mol^{-1}). The reason for this very good agreement is probably that the experimental conditions (especially the G6P initial molality) in Dyson's work and our work compare very well. Moreover, the $\Delta^R h^+$ value measured with ITC in our work ($\Delta^R h^+$ = 12.25 kJ mol^{-1}) compares well with $\Delta^R h^+$ obtained from temperature-dependent $\Delta^R g^+$ data from Dyson's work applying the van't Hoff equation ($\Delta^R h^+$ = 11.81 kJ mol^{-1}).

The availability of consistent data on $\Delta^R g^+$ and $\Delta^R h^+$ has a big impact also on non-equilibrium in-vivo reactions where especially $\Delta^R g^+$ is needed to determine the Gibbs energy of reaction $\Delta^R g$ that gives information on the feasibility of a reaction under real conditions (non-equilibrium metabolite concentrations).

5.2. Prediction of K_γ values with ePC-SAFT

According to Eq. (4), the thermodynamic equilibrium constant K_a and the apparent equilibrium constant K_m differ by the ratio of activity coefficients K_γ. In Section 5.1, experimental K_a values were determined by the extrapolation procedure described in Fig. 1, and K_m values were measured and also illustrated in Fig. 1. Thus, K_γ values are accessible in this work from these experimental K_m and K_a values, denoted by K^{exp}_γ. Alternatively, K_γ values can also be obtained from a thermodynamic model, denoted here by $K^{ePC\text{ - }SAFT}_\gamma$.

In order to predict K_γ values with ePC-SAFT, the ePC-SAFT parameters of each compound/species present in the considered reaction mixture as well as binary interaction parameters k_{ij} between water and a solute (e.g. the reacting agents $G6P^{2-}$, $F6P^{2-}$, or the species of the buffer Tris–HCl) have to be determined. If not yet available in the literature, these parameters were adjusted to reaction-independent phase-equilibrium data of pure components and binary water/solute solutions (see Appendix A for results). Based on these parameters (given in Table 4 in Appendix A), the activity coefficients of the reactant G6P ($\gamma^{*,m}_{G6P}$) and the product F6P ($\gamma^{*,m}_{F6P}$) of the isomerization were predicted at solution conditions (temperature, molality of $G6P^{2-}$, $F6P^{2-}$, and buffer species) as reported in Table 2. The experimental K^{exp}_γ as well as the ePC-SAFT predicted activity coefficients and the resulting $K^{ePC\text{ - }SAFT}_\gamma$ obtained using Eq. (6) are listed in Table 3.

Fig. 2 shows the experimental K^{exp}_γ and the predicted $K^{ePC\text{ - }SAFT}_\gamma$ values at 37 °C as function of the equilibrium molality of $G6P^{2-}$. It can be observed that the K_γ values starting from 1 at infinite dilution

Table 3
ePC-SAFT predicted activity coefficients of $G6P^{2-}$ and $F6P^{2-}$ ($\gamma_i^{*,m}$) as a function of the equilibrium molalities and temperatures (according to reaction batch Nos. 1–6 in Table 2), together with the resulting values for $K_\gamma^{ePC\text{-}SAFT}$ and the experimental values for K_γ^{exp}. The deviations AAD and ARD [in %] between the predicted and the experimental K_γ values were calculated with Eq. (11).

Batch	T [°C]	$\gamma^{*,m}_{G6P^{2-}}$	$\gamma^{*,m}_{F6P^{2-}}$	$K_\gamma^{ePC\text{-}SAFT}$[a]	K_γ^{exp}[b]	AAD[c]	ARD[c] [%]
1	25	0.9935	0.9915	0.998	1.034	0.036	3.48
	30	0.9938	0.9908	0.997	0.982	0.015	1.53
	37	0.9942	0.9906	0.996	0.979	0.017	1.74
2	25	0.9830	0.9767	0.994	1.009	0.015	1.49
	30	0.9839	0.9758	0.992	1.023	0.031	3.03
	37	0.9851	0.9742	0.989	0.972	0.017	1.75
3	25	0.9730	0.9609	0.988	0.959	0.029	3.02
	30	0.9744	0.9593	0.984	0.964	0.020	2.07
	37	0.9762	0.9581	0.982	0.972	0.010	1.03
4	25	0.9489	0.9222	0.972	0.907	0.065	7.17
	30	0.9517	0.9191	0.966	0.917	0.049	5.34
	37	0.9548	0.9178	0.961	0.937	0.024	2.56
5	25	0.9038	0.8504	0.941	0.881	0.060	6.81
	30	0.9096	0.8418	0.925	0.866	0.059	6.81
	37	0.9158	0.8377	0.915	0.871	0.044	5.05
6	25	0.7918	0.6615	0.835	0.808	0.027	3.34
	30	0.8063	0.6401	0.794	0.771	0.023	2.98
	37	0.8214	0.6263	0.762	0.752	0.010	1.33
				Average deviation:	25 °C	0.039	4.22
					30 °C	0.033	3.63
					37 °C	0.020	2.24

[a] Calculated using Eq. (6).
[b] Calculated using Eq. (4) with K_a and K_m from Section 1.
[c] Calculated using Eq. (13).

decrease to less than 0.8 at the highest considered $G6P^{2-}$ equilibrium molality, which corresponds to a relative decrease of more than 20%. Comparing K_γ^{exp} and the predicted $K_\gamma^{ePC\text{-}SAFT}$ values yields a very good agreement of the two values with an absolute relative deviation (ARD Eq. (11) of Appendix A) of only 2%. Nearly the same results were found also at 25 °C and 30 °C (results given in Table 3). This is an excellent result keeping in mind that ePC-SAFT was used to predict these values, i.e. the ePC-SAFT parameters were adjusted to reaction equilibrium-independent data only.

5.3. Influence of additives and pH on the G6P isomerization equilibrium

5.3.1. Influence of additives

The G6P isomerization equilibrium is affected not only by the G6P and F6P equilibrium molalities (as shown in Section 1) but also by the presence of inert additives. As the in-vitro equilibrium measurements are typically carried out in buffered solutions, the buffer (Tris–HCl in this work) can be considered as such a reaction additive. In contrast, in-vivo reactions occur under the presence of cellular compounds like salts or amino acids, which also can be considered as additives.

In this work, the influence of the Tris and potassium glutamate (KGlu) were investigated at $m_{G6P}^{init} = 0.05$ mol kg^{-1} and T = 37 °C. The Tris molality was varied in the range 0.01 < mol kg^{-1} Tris < 0.5. KGlu was added in the range 0.05 < mol kg^{-1} KGlu < 1. As shown in Fig. 3, increasing molalities of Tris or KGlu caused a decrease of K_m. That is, these additives shift the equilibrium backwards to the reactant side. At $m_{Tris} = 0.5$ mol kg^{-1}, K_m decreases to 0.464 (from 0.496 at $m_{Tris} = 0.01$ mol kg^{-1}). Nearly the same result was found for KGlu at $m_{KGlu} = 0.5$ mol kg^{-1}. Further addition of KGlu until $m_{KGlu} = 1$ mol kg^{-1} caused K_m to decrease even down to 0.433.

Considering the almost linear dependency of K_m on m_{Tris} and m_{KGlu}, the equilibrium shift will be more even pronounced at higher additive molalities. In particular for in-vitro equilibrium measurements where usually a buffer is present, the results emphasize the need for reporting also the exact buffer molality used. At in-vivo conditions, many additives might be present (molecular crowding)

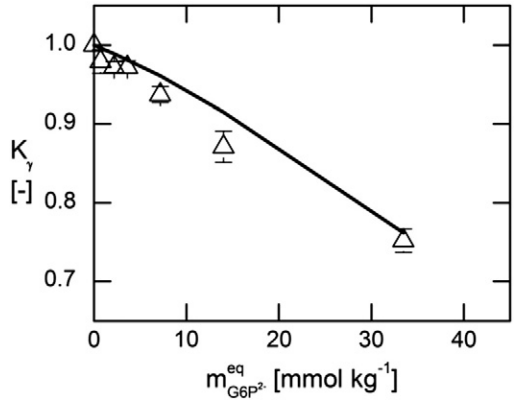

Fig. 2. Experimentally-determined K_γ values (K_γ^{exp}) obtained from equilibrium measurements (symbols) and ePC-SAFT predicted K_γ values ($K_\gamma^{ePC\text{-}SAFT}$) (line) at 37 °C as a function of the $G6P^{2-}$ equilibrium molality.

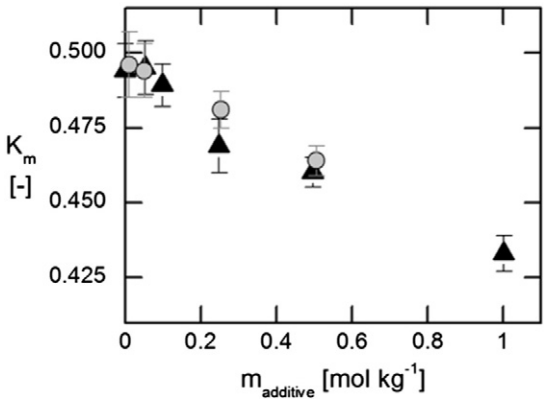

Fig. 3. Experimental apparent equilibrium constants K_m of the G6P isomerization as a function of the additive molality at $m_{G6P}^{init} = 0.05$ mol kg^{-1} and 37 °C. The influence of Tris–HCl (gray circles) and of KGlu (black triangles) on K_m was investigated.

showing the importance of accounting also for their influence on reaction equilibria.

The K_a value for the additive-free isomerization determined in Section 5.1 ($K_a = 0.372$ at 37 °C) was used to calculate experimental K_γ values using Eq. (4) and the K_m values shown in Fig. 3. As a result, the so-determined experimental K_γ^{exp} values are illustrated in Fig. 4. Fig. 4 shows that increasing the molality of Tris or of KGlu causes increased K_γ^{exp} values. K_γ^{exp} increases from 0.75 ($m_{Tris-HCl} = 0.01$ mol kg^{-1}) to 0.80 ($m_{Tris-HCl} = 0.5$ mol kg^{-1}) upon Tris addition. Adding 1 mol kg^{-1} KGlu causes K_γ even to increase from 0.75 (at $m_{KGlu} = 0$ mol kg^{-1}) to 0.86.

Again, also ePC-SAFT was used to predict K_γ as a function of Tris–HCl molality and KGlu molality. The required pure-component parameters for KGlu and the k_{ij} between water and KGlu were fitted to phase-equilibrium data of aqueous KGlu solutions. All parameters are summarized in Table 4 of Appendix A. The buffer Tris–HCl contains the species Tris, Tris–H^+, H^+, and Cl^-. The composition of the buffer depends on the pH of the solution. At the reaction conditions considered in this work, all four buffer species are present. The pure-component parameters of H^+ and Cl^- were taken from Held et al. [22]. The pure-component parameters of Tris and Tris–H^+ were fitted to phase-equilibrium data of aqueous solutions in which one of the species (Tris or Tris–H^+) were exclusively present. Details and results are given in Appendix A.

The result of the ePC-SAFT prediction can be also seen in Fig. 4. As before, the experimental K_γ^{exp} and the predicted $K_\gamma^{ePC\text{-}SAFT}$ values are in very good agreement. This demonstrates that ePC-SAFT is capable to predict the $G6P^{2-}$ and $F6P^{2-}$ activity coefficients (and thus $K_\gamma^{ePC\text{-}SAFT}$) also in the presence of Tris and KGlu. This is an excellent result, keeping in mind that K_γ^{exp} increases up to 15% upon addition of 1 molal additive (KGlu or Tris) and that the parameters have not been fitted to any reaction-equilibrium data.

Considering the molality range of Tris–HCl buffer and of the KGlu additive in Fig. 3, it shows that very high molalities of the two substances were investigated. We are aware of the fact that buffer molalities are often lower than 0.5 mol kg^{-1} in literature in-vitro equilibrium measurements. However, the concentration of additives might easily increase up to 300 g/l under in-vivo conditions. Thus, the presence of various biological additives with different sizes and charges is expected to have a huge influence on the $G6P^{2-}$ and $F6P^{2-}$ activity coefficients under in-vivo conditions. A significant influence of e.g. macromolecular additives is strongly suggested yet (molecular crowding) [33–36]. Accordingly, the influence of any compound (although moderate in some cases) on reaction equilibria cannot be a-priori considered to be negligible.

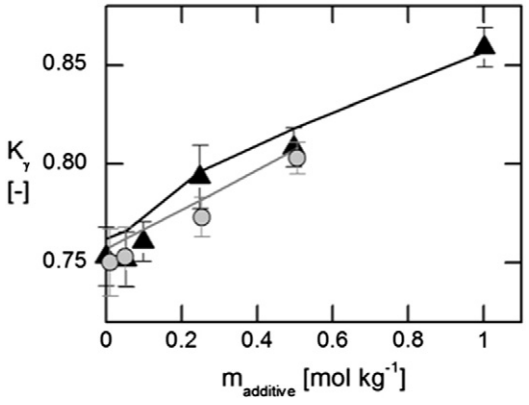

Fig. 4. Comparison of the experimentally-determined K_γ^{exp} values (symbols) from the equilibrium measurements and the ePC-SAFT predicted $K_\gamma^{ePC\text{-}SAFT}$ values (lines) as function of the Tris molality (gray circles) and of the KGlu molality (black triangles) at $m_{G6P}^{init} = 0.05$ mol kg^{-1} and T = 37 °C.

Table 4
ePC-SAFT pure-component parameters of all components involved in the G6P isomerization. The binary interaction parameters k_{ij} between the associating compounds and water are also shown.

Component	m_i^{seg}	σ_i	u_i/k_B	N_i^{assoc}	ε^{AiBi}/k_B	κ^{AiBi}	k_{ij} (H_2O)
$F6P^{2-}$ [a]	35.5936	1.8100	198.49	10 [c]	5000.0	0.100000	−0.065
$G6P^{2-}$ [a]	22.3290	2.2266	243.31	10 [c]	5000.0	0.100000	−0.065
KGlu [a]	8.6159	2.4388	269.83	2	7791.1	0.039180	−0.091
Tris [a]	6.3730	2.7484	302.16	2	4786.9	0.020271	−0.047
Tris–H^+ [a]	10.2047	2.4081	348.10	8	10970.9	0.000001	−0.052
Water [b]	1.2047	[d]	353.94	2	2425.7	0.045099	–
Cl^- [b]	1.0000	3.0575	472.88	–	–	–	–
K^+ [b]	1.0000	2.9698	271.05	–	–	–	–

[a] This work.
[b] Taken from [22].
[c] Taken from [39].
[d] $\sigma_{water} = 2.7927 + 10.11\exp(-0.01775\,T) - 1.417\exp(-0.01146\,T)$.

The activity-coefficient ratio K_γ cannot be assumed to be unity for the considered reaction. Neglecting K_γ thus causes a huge error in the determination of $\Delta^R g^+$. Comparing the influence of the reactants and products on K_γ (Fig. 2) with the influence of additives on K_γ (Fig. 4) this work shows that the influence of the reactant and product concentration on K_γ is the dominating effect.

5.3.2. Influence of pH

The pH value of the solution usually influences reaction-equilibrium data mainly due to the protonation state of the reacting species. As the pK_a values of $G6PK_2$ and $F6PK_2$ are similar and are both much lower than the pH of the investigated solutions, the reacting species $G6P^{2-}$ and $F6P^{2-}$ will not change their protonation state as long as $pH \gg pK_a$. Therefore, pH was not expected to influence the G6P isomerization. To proof that, K_m values were measured at pH 7.5 and compared to pH 8.5 in Tris–HCl buffer at 37 °C without further additives. It was found that the deviation between the K_m values at $7.5 \leq pH \leq 8.5$ was within the experimental error, which means that pH indeed has no effect on the equilibrium of the G6P isomerization.

Although pH variation between 7.5 and 8.5 has been shown to play a minor role on reaction equilibria in the G6P–F6P reaction, it is generally known that biological systems obey a complex pH behavior. Accounting for protonation/deprotonation of the sugar phosphates is thus of general importance. In case of reactions with reacting agents of very different pK_a values, variation of pH usually causes species diversity (protonated/deprotonated states) therewith influencing the activity-coefficient ratio of products and reactants dramatically. A huge influence of pH on reaction equilibria has been observed for e.g. the methyl ferulate reaction [15]. This can be assumed to occur also for all reaction steps of glycolysis (except G6P ↔ F6P) as the difference between the pK_a values of products and reactants in the glycolytic reactions are generally high.

6. Conclusions

In this work, the isomerization of glucose-6-phosphate to fructose-6-phosphate was investigated. Equilibrium measurements indicated that the apparent equilibrium constant K_m strongly depends on the initial G6P molality. This concentration dependence could be explained by non-unity activity coefficients of the reactant G6P and the product F6P.

These activity coefficients are accessible by thermodynamic models, e.g. ePC-SAFT. Fitting ePC-SAFT parameters to phase-equilibrium data only, allowed for predicting the activity coefficients of the reacting agents even in a multi-component system where reactant, product, solvent, and buffer species are explicitly accounted for.

The availability of activity coefficients allowed to calculate the true thermodynamic (concentration-independent) equilibrium constant K_a and therewith $\Delta^R g^+$. This work showed that the calculation of $\Delta^R g^+$ upon using either K_a or K_m differs by up to 30% for the considered

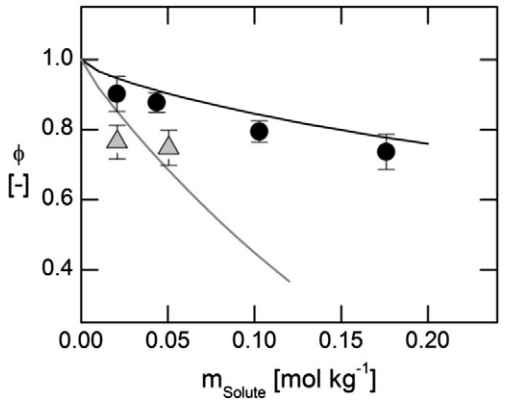

Fig. 5. Osmotic coefficients of $G6PK_2$/water (black) and $F6PK_2$/water solutions (gray) as a function of $G6PK_2$ and $F6PK_2$ molality at 0 °C. Experimental data are symbols, fitting results of the ePC-SAFT modeling are represented by the lines.

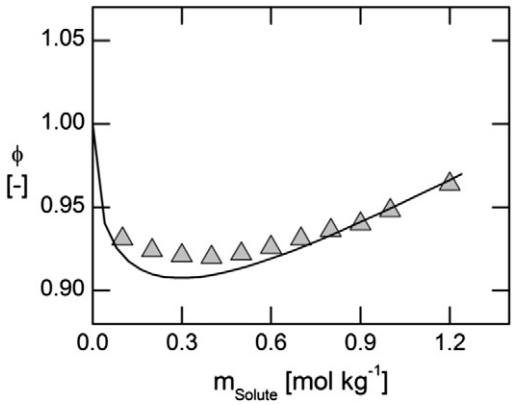

Fig. 7. Osmotic coefficients of KGlu/water solutions as a function of the solute molality at 25 °C. Experimental data are symbols from [38], fitting results of the ePC-SAFT modeling are represented by the line.

reaction. In fact, this clearly indicates that the activity coefficients cannot be neglected when determining $\Delta^R g^+$.

In order to validate experimental values measured in this work we compared the $\Delta^R h^+$ determined by ITC-calorimetry with $\Delta^R h^+$ obtained from temperature-dependent K_a values and applying the van't Hoff equation. As a result, both $\Delta^R h^+$ values differed in an absolute value of 0.2 kJ mol^{-1}, which corresponds to a deviation of 1.5% only. The benefit of this approach is bidirectional because it indicates the reliability of $\Delta^R h^+$ measured by ITC and the reasonability of the determination of K_a (extrapolation of K_m to zero reactant molality) and thus $\Delta^R g^+$.

Finally, it can be concluded that the influence of the substrate molality on the reaction equilibria of G6P ↔ F6P is much higher compared to the influence of additives. This could be explained by the activity coefficient ratio K_γ, which depends dramatically on the ratio of substrate and product. Upon the addition of non-reacting agents, the single activity coefficients of substrates and products might be considered equally effected, thus only moderately affecting the activity-coefficient ratio of substrate and product.

Investigations on the behavior of K_m values upon pH changes showed that K_m is independent of the pH of the solution between pH 7.5 and pH 8.5. This weak pH-dependence could be explained by the chemical similarity (equal pK_a values) of substrate and product. A much higher influence of pH on reaction equilibria can be expected for the other glycolytic reactions.

The results of this work indicate the significance to account for reactant and product activity coefficients for a correct thermodynamic analysis of biological reactions. Moreover, this study is meant to contribute to a further understanding of the G6P isomerization as part of glycolysis by including correct thermodynamic quantities. It is considered worthwhile to extend this kind of investigation also to other glycolytic reactions. The corresponding results are expected to provide a comprehensive database on K_a values and activity-coefficient data of the reactions and reactants of glycolysis, respectively.

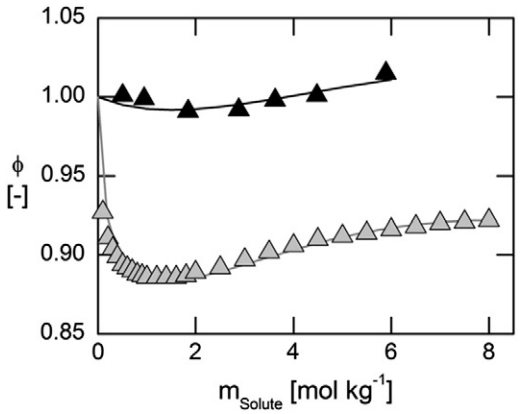

Fig. 6. Osmotic coefficients of Tris/water (black) and Tris–HCl/water (gray) solutions as a function of the solute molality at 25 °C. Experimental data are symbols from [37], fitting results of the ePC-SAFT modeling are represented by the lines.

List of symbols

Roman symbols		
a_i	[–]	activity of compound i
a	[J mol^{-1}]	Helmholtz energy
$\Delta^R g$	[J mol^{-1}]	Gibbs energy of reaction
$\Delta^R g^+$	[J mol^{-1}]	standard Gibbs energy of reaction
k_B	[J K^{-1}]	Boltzmann constant, 1.38065 · 10^{-23} J K^{-1}
k_{ij}		binary interaction parameter
K_a	[–]	activity-based (thermodynamic) equilibrium constant
K_γ	[–]	activity-coefficient ratio
K_m	[–]	molality-based equilibrium constant
m_i	[mol kg^{-1}]	molality (moles solute i per kg water)
m_i^{seg}	[–]	number of segments
M	[g mol^{-1}]	molecular weight
N	[–]	total number of molecules
N_i^{assoc}	[–]	number of association sites
NP	[–]	number of data points
R	[J mol^{-1} K^{-1}]	ideal gas constant, 8.31446 J mol^{-1} K^{-1}
T	[K]	temperature
u_i/k_B	[K]	dispersion-energy parameter
y	[–]	measured value
Greek symbols		
ε^{AiBi}/k_B	[K]	association-energy parameter
γ_i^*	[–]	rational activity coefficient of compound i (related to infinite dilution)
κ^{AiBi}	[–]	association-volume parameter
ν_i	[–]	stoichiometric factor of compound i
ϕ	[–]	osmotic coefficient
σ_i	[Å]	temperature-independent segment diameter of molecule i

Subscripts	
a	based on activity
exp	experimental
i, j, k	compound indices
m	based on molality
mod	modeled with ePC-SAFT
seg	segment
Superscripts	
assoc	association
disp	dispersion
eq	equilibrium
exp	experimental
hc	hard chain

(continued on next page)

init	initial
ion	ionic interaction
m	based on molality
res	residual
*	related to infinite dilution

Abbreviations

AAD	absolute average deviation
ARD	absolute average relative deviation
CAS	chemical abstracts service
EC	enzyme commission
ePC-SAFT	electrolyte Perturbed-Chain Statistical Associating Fluid Theory
F6P	fructose-6-phosphate
G6P	glucose-6-phosphate
HPLC	high performance liquid chromatography
KGlu	potassium glutamate
NIST	National Institute of Standards and Technology
Tris	Trizma® base

Acknowledgments

The research leading to these results has received funding from the Ministry of Innovation, Science and Research of North Rhine-Westphalia in the frame of CLIB-Graduate Cluster Industrial Biotechnology, contract no: 314-108 001 08. The authors are very grateful for the contributions to this work by Sultan Mohammad, Matthias Voges, Matthias Heitmann, and Martina Effenberger.

Appendix A. Estimation of model parameters for ePC-SAFT

ePC-SAFT requires five pure-component parameters to model water, $G6P^{2-}$, $F6P^{2-}$, Tris, and KGlu, all of which were treated as associating molecules capable of forming hydrogen bonds (see Section 4). Only two parameters (the hydrated-ion diameter σ_{ion} and the dispersion-energy parameter u_{ion}/k_B) are required to model the inorganic ions H^+, K^+ and Cl^-. Whereas the model parameters for these ions [22] and for water [27] were already available, the parameters for G6P, F6P, Tris, Tris–H^+, and KGlu were not yet available and thus were determined in this work. The pure-compound PC-SAFT parameters are given in Table 4. The osmotic-coefficient measurements of all binary solute/water solutions were performed using an Osmomat 030 cryoscopic osmometer (Gonotec, Berlin, Germany), as described previously [28]. Prior to each measurement, the osmometer was calibrated with calibration standards of defined molality as provided by the supplier. The experimental results are shown in Fig. 5.

According to the literature pK_a values, only the twofold deprotonated species $G6P^{2-}$ and $F6P^{2-}$ will be present in the reaction mixtures in the experiments at pH ≥ 7.5. Accordingly, only the pure-component parameters for the species $G6P^{2-}$ and $F6P^{2-}$ were required. These parameters were also fitted to osmotic-coefficient and density data of binary $G6PK_2$/water and $F6PK_2$/water solutions measured in this work. The existence of potassium in the samples (see Table 2) was explicitly accounted for in the modeling (in the parameter estimation of $G6P^{2-}$ and $F6P^{2-}$ as well as in the prediction of K_γ values).

Modeling mixtures with ePC-SAFT requires mixing rules which were used according to Lorentz and Berthelot:

$$\sigma_{ij} = 0.5\left(\sigma_i + \sigma_j\right) \tag{10}$$

and

$$u_{ij} = \left(u_i u_j\right)^{0.5}\left(1-k_{ij}\right). \tag{11}$$

The binary k_{ij} parameter in Eq. (11) is introduced to correct for deviations from the mean in the dispersion-energy parameter between two components. All binary interaction parameters between solute and water were also fitted to the osmotic-coefficient data of the binary solutions. All binary interaction parameters between solutes or ion and solute were set to zero. The results are listed in Table 4.

The modeling results for the osmotic coefficients are shown in Fig. 5 (results for densities not reported).

It can be observed from Fig. 5 that the osmotic coefficients strongly decrease at low $G6P^{2-}$ and $F6P^{2-}$ molalities. Moreover, a stronger initial decrease of $\phi_{F6P^{2-}}$ compared to $\phi_{G6P^{2-}}$ can be observed. Since molalities higher than 0.1 mol kg^{-1} are usually of little interest for the investigation of bioreaction equilibria, a high accuracy for the parameter estimation at low molalities was emphasized in this study. As shown in Fig. 5, ePC-SAFT is capable of representing the experimental data reasonably well using the fitted parameters. The parameters of $G6P^{2-}$ and $F6P^{2-}$ are summarized in Table 4.

In contrast to $G6P^{2-}$ and $F6P^{2-}$, the buffer compound Tris–HCl ($pK_a = 8.3$ according to [30]) may occur in the deprotonated species (Tris) as well as in the protonated species (Tris–H^+) in the prepared reaction mixtures. The exact composition of the buffer depends on the pH and is given by the buffer equilibrium (Eq. (12)). In this work, this was accounted in the model by determining a pure-component parameter set for the Tris species and for the Tris–H^+ species.

$$\text{Tris} + H^+ \rightleftharpoons \text{Tris–}H^+ \tag{12}$$

The parameters for Tris were fitted to osmotic coefficients of Tris/water solutions (pH > 10) [37], since ≥99% of the initial Tris amount is present as the deprotonated species if only the base is dissolved in water. The parameters for Tris–H^+ were fitted to osmotic coefficients of Tris–HCl/water solutions (pH < 5) with an equimolar concentration of Tris and HCl [37]. At this pH, Tris–H^+ is the only existing Tris species. The quality of the fit for Tris and Tris–H^+ is demonstrated in Fig. 6. As shown, ePC-SAFT is capable to represent the experimental data very well.

The parameters for the reaction additive KGlu have also been fitted to osmotic-coefficient data of binary KGlu/water solutions [38] and could be represented reasonably well with ePC-SAFT (Fig. 7).

The absolute average deviations (AADs) and the absolute relative deviations (ARDs) between the experimental (exp) and the modeled (mod) osmotic coefficients are 0.042 and 5.1% for G6P, 0.076 and 10% for F6P, 0.003 and 0.3% for Tris, 0.003 and 0.3% for Tris–H +, and 0.006 and 0.7% for KGlu, respectively. AAD and ARD were calculated using the following equations:

$$\text{AAD} = \frac{1}{NP}\sum_{k=1}^{NP}\left|\left(y_k^{mod} - y_k^{exp}\right)\right|$$

and

$$\text{ARD} = 100\cdot\frac{1}{NP}\sum_{k=1}^{NP}\left|\left(1-\frac{y_k^{mod}}{y_k^{exp}}\right)\right| \tag{13}$$

where y represents the considered quantity (e.g., the osmotic coefficient).

Table 4 summarizes the pure-component parameters of all species and compounds involved in the PGI isomerization as described in this work. In addition, the values of the binary interaction parameters k_{ij} between the species or compounds and water are listed.

References

[1] T. Maskow, U. von Stockar, How reliable are thermodynamic feasibility statements of biochemical pathways? Biotechnol. Bioeng. 92 (2005) 223–230.
[2] R. Schuster, S. Schuster, Refined algorithm and computer program for calculating all non-negative fluxes admissible in steady states of biochemical reaction systems with or without some flux rates fixed, Bioinformatics 9 (1993) 79–85.
[3] H.P.J. Bonarius, G. Schmid, J. Tramper, Flux analysis of underdetermined metabolic networks: the quest for the missing constraints, Trends Biotechnol. 15 (1997) 308–314.

[4] K.C. Soh, V. Hatzimanikatis, Network thermodynamics in the post-genomic era, Curr. Opin. Microbiol. 13 (2010) 350–357.
[5] D.A. Beard, S.-d. Liang, H. Qian, Energy balance for analysis of complex metabolic networks, Biophys. J. 83 (2002) 79–86.
[6] H. Qian, D.A. Beard, S.-d. Liang, Stoichiometric network theory for nonequilibrium biochemical systems, Eur. J. Biochem. 270 (2003) 415–421.
[7] A. Kümmel, S. Panke, M. Heinemann, Putative regulatory sites unraveled by network-embedded thermodynamic analysis of metabolome data, Mol. Syst. Biol. 2 (2006).
[8] C.S. Henry, M.D. Jankowski, L.J. Broadbelt, V. Hatzimanikatis, Genome-scale thermodynamic analysis of *Escherichia coli* metabolism, Biophys. J. 90 (2006) 1453–1461.
[9] C.S. Henry, L.J. Broadbelt, V. Hatzimanikatis, Thermodynamics-based metabolic flux analysis, Biophys. J. 92 (2007) 1792–1805.
[10] M.L. Mavrovouniotis, Identification of localized and distributed bottlenecks in metabolic pathways, Proc. Int. Conf. Intell. Syst. Mol. Biol. 1 (1993) 275–283.
[11] M.L. Mavrovouniotis, Identification of qualitatively feasible metabolic pathways, Artif. Intell. Mol. Biol. (1993) 325–364.
[12] P. De Noronha Pissarra, J. Nielsen, Thermodynamics of metabolic pathways for penicillin production: analysis of thermodynamic feasibility and free energy changes during fed-batch cultivation, Biotechnol. Prog. 13 (1997) 156–165.
[13] I. Famili, J. Förster, J. Nielsen, B.O. Palsson, *Saccharomyces cerevisiae* phenotypes can be predicted by using constraint-based analysis of a genome-scale reconstructed metabolic network, Proc. Natl. Acad. Sci. 100 (2003) 13134–13139.
[14] J. Villadsen, J. Nielsen, G. Lidén, Thermodynamics of Bioreactions, In: Bioreaction Engineering Principles, Springer US, Boston, MA, 2011.
[15] P. Hoffmann, M. Voges, C. Held, G. Sadowski, The role of activity coefficients in bioreaction equilibria: thermodynamics of methyl ferulate hydrolysis, Biophys. Chem. 173–174 (2013) 21–30.
[16] J.E. Ladbury, B.Z. Chowdhry, Sensing the heat: the application of isothermal titration calorimetry to thermodynamic studies of biomolecular interactions, Chem. Biol. 3 (1996) 791–801.
[17] T. Maskow, H. Harms, Real time insights into bioprocesses using calorimetry: state of the art and potential, Trends Calorim. 6 (2006) 266–277.
[18] M.L. Bianconi, Calorimetry of enzyme-catalyzed reactions, Biophys. Chem. 126 (2007) 59–64.
[19] K.S. Pitzer, Thermodynamics of electrolytes. I. Theoretical basis and general equations, J. Phys. Chem. 77 (1973) 268–277.
[20] M. Sadeghi, C. Held, A. Samieenasab, C. Ghotbi, M.J. Abdekhodaie, V. Taghikhani, G. Sadowski, Thermodynamic properties of aqueous salt containing urea solutions, Fluid Phase Equilib. 325 (2012) 71–79.
[21] L.F. Cameretti, G. Sadowski, J.M. Mollerup, Modeling of aqueous electrolyte solutions with Perturbed-Chain Statistical Associated Fluid Theory, Ind. Eng. Chem. Res. 44 (2005) 3355–3362 ibid., 8944.
[22] C. Held, L.F. Cameretti, G. Sadowski, Modeling aqueous electrolyte solutions — part 1. Fully dissociated electrolytes, Fluid Phase Equilib. 270 (2008) 87–96.
[23] C. Held, G. Sadowski, Modeling aqueous electrolyte solutions. Part 2. Weak electrolytes, Fluid Phase Equilib. 279 (2009) 141–148.
[24] J. Gross, G. Sadowski, Perturbed-Chain SAFT: an equation of state based on a perturbation theory for chain molecules, Ind. Eng. Chem. Res. 40 (2001) 1244–1260.
[25] C. Held, T. Neuhaus, G. Sadowski, Compatible solutes: thermodynamic properties and biological impact of ectoines and prolines, Biophys. Chem. 152 (2010) 28–39.
[26] C. Held, L.F. Cameretti, G. Sadowski, Measuring and modeling activity coefficients in aqueous amino-acid solutions, Ind. Eng. Chem. Res. 50 (2011) 131–141.
[27] D. Fuchs, J. Fischer, F. Tumakaka, G. Sadowski, Solubility of amino acids: influence of the pH value and the addition of alcoholic cosolvents on aqueous solubility, Ind. Eng. Chem. Res. 45 (2006) 6578–6584.
[28] C. Held, A. Prinz, V. Wallmeyer, G. Sadowski, Measuring and modeling alcohol/salt systems, Chem. Eng. Sci. 68 (2012) 328–339.
[29] C. Held, G. Sadowski, A. Carneiro, O. Rodríguez, E.A. Macedo, Modeling thermodynamic properties of aqueous single-solute and multi-solute sugar solutions with PC-SAFT, AIChE J. 59 (2013) 4794–4805.
[30] T. Pan, A. Hashimoto, M. Kanou, K. Nakanishi, T. Kameoka, Development of a quantification system of ionic dissociative metabolites using an FT-IR/ATR method, Bioprocess Biosyst. Eng. 26 (2003) 133–139.
[31] H.P. Smits, A. Cohen, T. Buttler, J. Nielsen, L. Olsson, Cleanup and analysis of sugar phosphates in biological extracts by using solid-phase extraction and anion-exchange chromatography with pulsed amperometric detection, Anal. Biochem. 261 (1998) 36–42.
[32] R.N. Goldberg, Y.B. Tewari, T.N. Bhat, Thermodynamics of enzyme-catalyzed reactions — a database for quantitative biochemistry, Bioinformatics 20 (2004) 2874–2877.
[33] R.J. Ellis, Macromolecular crowding: an important but neglected aspect of the intracellular environment, Curr. Opin. Struct. Biol. 11 (2001) 114–119.
[34] A.P. Minton, Molecular crowding: analysis of effects of high concentrations of inert cosolutes on biochemical equilibria and rates in terms of volume exclusion, in: A. P. Minton (Ed.), Methods in Enzymology, Elsevier, 1998, pp. 127–149.
[35] A.P. Minton, The influence of macromolecular crowding and macromolecular confinement on biochemical reactions in physiological media, J. Biol. Chem. 276 (2001) 10577–10580.
[36] A.P. Minton, How can biochemical reactions within cells differ from those in test tubes? J. Cell Sci. 119 (2006) 2863–2869.
[37] R.A. Robinson, V.E. Bower, Osmotic and activity coefficients of tris(hydroxymethyl) aminomethane and its hydrochloride in aqueous solution at 25 °C, J. Chem. Eng. Data 10 (1965) 246–247.
[38] O.D. Bonner, Osmotic and activity coefficients of sodium and potassium glutamate at 298.15 K, J. Chem. Eng. Data 26 (1981) 147–148.
[39] A.P. Carneiro, C. Held, O. Rodriguez, G. Sadowski, E.A. Macedo, Solubility of sugars and sugar alcohols in ionic liquids: measurement and PC-SAFT modeling, J. Phys. Chem. B 117 (2013) 9980–9995.
[40] R. Garrett, C.M. Grisham, Biochemistry, 3rd ed.Thomson Brooks/Cole, Belmont, CA, 2005, pp. 582–583.
[41] J.E.D. Dyson, E.A. Noltmann, The effect of pH and temperature on the kinetic parameters of phosphoglucose isomerase, J. Biol. Chem. 243 (1968) 1401–1414.